Response to Referee #1

Main comments:

(1) In the "Experimental procedure" it is not clear how many experiments were performed (it is ambiguous for the blank experiments and missing for the experiments themselves). The authors should clearly state upon how many replicates are based their conclusions and provide a table for various initial conditions and main results.

The paper is based on the results of 51 chamber characterization experiments and 7 field test experiments. The characterization experiments include15 blank/contamination related experiments, 14 experiments characterizing wall losses, 6 experiments quantifying the ambient air sampling efficiency, 3 experiments for the measurement of J_{NO2}, 9 experiments related to RH and UV variations, and 4 VOC loss experiments. A table with the details of these experiments has been added to the Supplementary Information of the revised manuscript. The number of experiments on which the various conclusions are based is now clearly stated.

(2) Sometimes, the analysis is oversimplified. Some key measurements are not given (see below my comments) and the literature survey is not wide enough.

We have followed the reviewer's suggestion and extended the literature survey (including those in Comments 3 and 4). In the original paper we focused on the historical development of smog chamber experiments. We now include more smog chamber studies focusing on their methodological contributions. We have also added information about the suggested measurements. Additional experiments have been performed during the revision stage to better characterize the behavior of the chamber with respect to the NO, NO_2, and O_3 losses to the walls and OH production.

(3) The authors should have tried to better define the behavior of the chamber walls toward the NOx/air/light system. This is a valuable exercise which is required for most of the chamber application. This is especially important since HONO was used as a source of OH radicals. They should perform deeper analysis and to build an auxiliary mechanism made of pseudo-elementary reactions with rate constants parameterized upon their experimental data. See for instance: Jeffries et al., 1976; Akimoto et al., 1979; Bloss et al., 2005; Carter et al., 2005; Hynes et al., 2005; Rohrer et al., 2005, Metzger et al., 2008; Wang et al, 2011; Wang et al, 2014.

We have performed additional experiments characterizing the losses of NO, NO_2, and O_3 to the walls of the chambers as well as the OH production. These are described in the revised paper. A basic auxiliary mechanism has been developed and has been to the paper.

(4) Previous simulation chamber studies observed a significant background OH production that could not be attributed to known OH radical precursors (Rohrer et al., 2005). A heterogeneous formation of HONO and its subsequent photolysis was suggested to explain this so called "background reactivity" within simulation chambers (Akimoto et al., 1987; Carter et al., 1982;

Glasson and Dunker, 1989; Killus and Whitten, 1990; Sakamaki and Akimoto, 1988). It was postulated that HONO is formed by the heterogeneous dark hydrolysis of NO_2 on the humid chamber surfaces (see for example Carter et al., 1982; Finlayson- Pitts et al., 2003; Jenkin et al., 1988; Kleffmann et al., 1998; Pitts et al., 1984; Sakamaki et al., 1983; Svensson et al., 1987) the mechanisms of which are still under discussion. Did the authors calculated the ratio of HONOwalls/HONOinjected. This background HONO production could differ at varying lightning conditions. Higher light intensities as it is the case in this study ($J(NO_2) = 0.1\ min^{-1}$) would increase the quasi-stationary background OH concentrations. More significant HONO and OH background production rates can only be determined by especially dedicated experiments including systematic variations of RH and light intensity.

Following the reviewer's suggestion, we performed several additional experiments focusing on the production of OH due to the walls as a function of RH and light intensity. The OH levels were estimated by the decay of d-butanol that was added to the clean chambers. Assuming pseudo-steady state for the OH radicals we then estimated their effective production rate. The production rate was practically negligible at low RH but it did increase at 50% and depended on light intensity. These results are described in the revised paper. The OH produced from our HONO injection, and not the OH due the walls, is the dominant source of OH in our perturbation experiments. One important note for our experiments is that because d-butanol is injected in all of them, the OH is estimated directly and therefore the OH exposure reported is already taking into account the wall source.

(5) There is no information about the estimated water quantity adsorbed on the Teflon wall or about the VOCs adsorbed on the wall. As mentioned above the blank experiments can lead to a HONO production from the chamber walls. What could be the zero order constant in ppt/s of HONO production from the chamber walls? The photolytic wall source of HONO is proportional to the J_{NO2} (Rohrer et al., 2005) and somewhat related with the NO_2 concentration (for example Hynes et al., 2005 or Wang et al, 2011or Wang et al, 2014).

We have performed vapor loss experiments for a few selected VOCs. The loss rates were quite low (less than 1 percent per hour). These results have been added to the revised paper. The estimation of the water adsorbed on the Teflon walls of our chambers is not possible right now. As discussed in our responses to Comment 4 we have performed additional experiments to quantify the magnitude of the wall OH source. Our estimated HONO production rate is less than 1 ppt/s for the J_{NO2} and RH ranges used in this study. This information has been added to the revised paper.

Minor comments

(6) What is the mixing ratio of HONO introduced in the chamber?

HONO was not measured directly. The concentration of OH was estimated in all experiments by the decay of d-butanol over time. The estimated levels are of the order of 100 ppb.

(7) As the wall material seems to have a significant importance, please provide the precise reference of the material: producer, ref number, and product name.
We used DuPont PTFE 2 mil, 0.5 m wide to construct the chambers. This information has been added to the revised manuscript.

(8) As the Teflon foil is new and used just before the preliminary experiments how the blank experiments were distributed during the campaign? If, they were evenly distributed among experiments, did you notice any evolution of the wall chemical behavior?
The chambers were built by us in our laboratory in Patras and were thoroughly cleaned and conditioned before the characterization experiments. Their cleaning procedure involved first passing of high O_3 concentrations with the UV lights on and heating to approximately 50^{o}C. Clean air passed then through chambers for several hours. A blank experiment was performed every few experiments both in the lab (during the characterization phase) and in the field. The wall losses are measured in each field experiment. We did not observe any evolution of the wall chemical behavior in these initial tests, but it something that we will keep investigating in future work.

(9) Adsorbed organics on the chamber wall can also come from the foil production process (see Carter et al, 1982 for example), it is hence not relevant to only refer to the level of VOCs coming from the ambient air.
This is correct, so we have rephrased the corresponding sentence. We did our best to clean the walls after the construction of the chambers from any residue of the Teflon production process (see also our response to Comment 8) but some volatile or semivolatile material could be still in theory present.

1

Response to Referee #2

(1) Line 105. Six panels with 36 UV lights are used to allow photo-oxidation experiments resulting in a J(NO2) of 0.1 min^{-1}. How does this number compare with other indoor chambers? I think it would be useful for readers if a UV-Vis spectrum of the lamps would be added as a figure.

The J_{NO2} in indoor atmospheric simulation chambers covers a wide range from zero (several metal chambers do not have lights) to as much as 1 min^{-1}. We have added the corresponding information in the revised paper. We have added a spectrum of the lamps in the Supplementary information. It peaks in the 350-400 nm region.

(2) Line 128. A compressor is used to provide clean air and an activated carbon and silica gel denuders are used to purify the compressed air before introduction into the chamber. How efficient were these denuders to remove O_3 and VOCs? Is NOx efficiently removed by this set up?

Please note that the compressor and air cleaning system is not used for the actual experiments. In these experiments the chambers are filled with ambient air without the use of a cleaning devices. The compressor/cleaning system is used for the cleaning of the chambers between experiments and for blank or other chamber characterization experiments. This is now clarified in the paper.

Typically, the concentrations of ozone, NOx and larger VOCs values are below or close to the detection limit in the chambers when they are filled with clean air from our system. The scrubbers were replaced regularly and the residence time inside them was kept as high as possible (maintaining the corresponding flow rates as low as possible). The concentrations of some of the small oxygenated VOCs such as acetone, acetic acid and methanol were slightly elevated compared to the cylinder zero air. The above information has been added to the revised manuscript.

(3) Line 185. Please describe the meaning of the "theta angle", which is used several times in the paper, for the non-specialist reader.

The theta angle is a measure of the similarity of the OA spectra (similar to the often used R^2). It treats each mass spectrum as a vector (each *m*/*z* is an element of the vector) and expresses the angle between two such spectra. We prefer to use theta angle for AMS spectra comparisons because it can distinguish small differences that the coefficient of determination cannot. The above explanation has been added to the revised manuscript.

(4) Line 193. Are the significant losses of particles < 80 nm mainly occurring in the pump? How long is the tubing from the inlet to the chambers?

The length of the tubing is approximately one meter (with a 0.5-inch diameter). The estimated losses for this tube for the flow rates used and for particles in the 20-80 nm size range are 1-3 percent. Therefore, most of the losses are indeed due to the pump. The above information has been added to the revised manuscript.

(5) Line 216. Why was the particle loss rate constant over the measured particles sizes in the lab experiments but shows a strong size dependence in field experiments?

During the field deployment of the chambers the induced friction of the walls and the handling resulted in higher charges on the chambers walls resulting in higher particle wall losses. On the other hand, when the chambers were inside the lab, there was no build-up of charges and the losses were lower. We have recently presented a detailed analysis of the losses of particles on our Teflon chambers (both the laboratory and the field ones) in Wang et al. (2018). A brief summary of these results and the corresponding reference have been added.

(6) Figure 5. This control experiment demonstrates that an entirely deflated chamber caused larger wall losses of particles. Does this result affect the standard field operation of the chambers? Are they transported to the field partially inflated?

The high particle wall losses introduce uncertainty in the results, because the wall-loss corrections dominate the corrected concentration values. If the losses are very high, the maximum duration of such experiments may be limited. We have been working on developing methods to minimize these effects. Moving the chambers to the field site either fully or at least partially inflated inside our mobile laboratory clearly helps. We have also been exploring other means of reducing these surface changes in the field. A brief discussion of this topic has been added.

(7) Figure 9 and 10. I recognize that this is a chamber characterization paper but it would be nice if the authors could add a few more thoughts on the interpretation of the measurements they present in figures 9 and 10. How significant are the changes observed? How do these changes compare to organic aerosol evolution in the ambient atmosphere or with "normal" SOA chamber experiments?

We have followed the reviewer's suggestion and added some more discussion about the measurements shown in these two figures. The results of several such ambient air experiments with detailed analysis of the formed aerosol, comparison with ambient and laboratory measurements are included in a forthcoming publication.

A portable dual smog chamber system for atmospheric aerosol field studies

Christos Kaltsonoudis[1,2,3], Spiro D. Jorga[3], Evangelos Louvaris[1,2], Kalliopi Florou[1,2] and Spyros N. Pandis[1,2,3]

[1]Institute of Chemical Engineering Sciences, ICE-HT, Patras, Greece
[2]Department of Chemical Engineering, University of Patras, Patras, Greece
[3]Department of Chemical Engineering, Carnegie Mellon University, Pittsburgh, USA

Abstract

Smog chamber experiments using as a starting point ambient air can improve our understanding of the evolution of atmospheric particulate matter at timescales longer than those achieved by traditional laboratory experiments. These types of studies can take place under more realistic environmental conditions addressing the interactions among multiple pollutants. The use of two identical smog chambers, with the first serving as the baseline chamber and the second as the perturbation chamber (in which addition or removal of pollutants, addition of oxidants, change in the relative humidity, etc.), can facilitate the interpretation of the results in such inherently complex experiments. The differences of the measurements in the two chambers can be used as the basis for the analysis of the corresponding chemical or physical processes of ambient air.

A portable dual smog chamber system was developed using two identical pillow-shaped smog chambers (1.5 m^3 each). The two chambers are surrounded by UV lamps in a hexagonal arrangement yielding a total J_{NO2} of 0.1 min^{-1}. The system can be easily disassembled and transported enabling the study of various atmospheric environments. Moreover, it can be used with natural sunlight. The results of test experiments using ambient air as starting point are discussed as examples of applications of this system.

1. Introduction

Teflon reactors, known as smog or atmospheric simulation chambers have been valuable research tools for the study of the complex chemical interactions that take place in the atmosphere. Studies using such reactors date back to the 1950s (Finlayson and Pitts, 1976). The use of these chambers eliminates many of the uncertainties resulting from the analysis of ambient

observations where several variables, such as weather conditions, pollutant emission rates, dilution and transport are all contributing to the observed changes (Kim et al., 2009). Typically, these reactors are made of Teflon, though there are some chambers that are made of metal or glass (Cocker et al., 2001a; Paulsen et al., 2005; Kim et al., 2009). The volume of these chambers varies from a few hundred liters up to hundreds of cubic meters, with the larger configurations having lower surface to volume ratio, thus minimizing the wall effects (Cocker et al., 2001a).

Chambers are placed either indoors or outdoors with the former having the advantage of a well-controlled environment with constant temperature, light intensity etc. and the latter being able to use natural sunlight (Laity, 1971; Jeffries et al., 1976; Leone et al., 1985; Carter et al., 2005). For the indoor chambers, a variety of UV light sources can be used including black light lamps (Laity, 1971), xenon, and argon arc lamps (Warren et al., 2008). The J_{NO2} in indoor atmospheric simulation chambers covers a wide range from zero (several metal chambers do not have lights) to as much as around 1 min^{-1} (Kim et al., 2009). Some chamber facilities include two identical smog chambers in order to use the first chamber as a reference (Kim et al., 2009). This practice can enhance the quality of the results since numerous variables can have an effect on the outcome of each experiment.

Different groups around the world have conducted thousands of smog chamber experiments in order to simulate the behavior of pollutants in ambient air. These smog chambers have been used to study, for example, secondary organic aerosol and its dependence on temperature, relative humidity, UV intensity, NO_x levels, etc. (Halquist et al., 2009; Tritscher et al., 2011). Other studies have focused on the characterization and evolution of primary emissions from selected sources (Weitkamp et al., 2007; Kostenidou et al., 2013; Platt et al., 2013).

There have been a number of studies that used ambient air as the starting point of the experiment. Roberts and Friedlander (1976) added SO_2, 1-heptene and NO_x to a 96m^3outdoor chamber filled with ambient air to study the aerosol formation. Heisler et al. (1977) used ambient air to fill an outdoor 80 m^3 Teflon chamber to study the growth rate of the particles. Pitt et al. (1977) concluded that the addition of N,N'-diethylhydroxylamine in ambient air enhances the formation of ozone, peroxyacetyl nitrate, and light-scattering particles. Kelly (1987) used a 0.5 m^3 chamber to investigate the HNO_3 formation in ambient air. Kelly and Gunst (1990) studied the ozone dependence on hydrocarbons and nitrogen oxide using ambient air. Lee et al. (2010)

investigated the correlations between light intensity and ozone formation for ambient air in Seoul. The potential OA enhancement or sink due to aging of ambient air has been also studied in the field by the use of oxidation flow reactors (OFR) in various ambient environments (Tkacik et al., 2014; Ortega et al., 2016). The OFR uses high OH levels, thus simulating atmospheric oxidation in timescales of several days to weeks. On the other hand, typical experiments in atmospheric simulation chambers take place at close to ambient OH levels and simulate hours to a few days of aging.

There have been a few efforts to use portable smog chamber facilities for different applications. For example, Shibuya et al. (1981) used a portable 4.5 m^3 smog chamber, installed in a vehicle, to study the ozone formation in ambient air. Hennigan et al. (2011) and Stockwell et al. (2014) developed portable twin-chamber systems with UV lights to monitor the aging of combustion emissions. A portable smog chamber facility was also developed by Platt et al. (2013) featuring a 9 m^3 Teflon reactor that can be mounted on a trailer.

The interactions of the walls of the chamber with the pollutants inside it represent a major experimental challenge and have been the topic of several studies. Gas-phase pollutants (e.g., ozone) are lost to the walls and increased relative humidity tends ~~Nitrogen oxide (NO), nitrogen dioxide (NO_2) and ozone (O_3) concentrations have been studied in chambers in order to extract decay rates related to background reactivity of the chamber walls. Generally humidified air tends~~ to increase the decay rates measured (Akimoto et al., 1979). The walls also can serve as a source of ~~Background reactivity of the chamber systems has also been studied especially in respect to the~~ OH mainly outgassing ~~production due to~~ nitrous acid (HONO) ~~out-gassing amongs other sources from the chamber walls~~ (Jeffries et al., 1976; Akimoto et al., 1979; Carter et al., 1982; Sakamaki et al., 1983; Pitts et al., 1984; Jenkin et al., 1987; Glasson and Dunker, 1989; Killus and Whitten, 1990; Finlayson-Pitts et al., 2003). In most cases~~,~~ OH production increases with temperature, humidity and~~,~~ NO_2 ~~concetration~~concentration ~~and light intensity~~ (~~.~~ Sakamaki et al., 1983; Pitts et al., 1984~~; and~~ Kleffmann et al.,1998; ~~studiedthe heterogeneous reaction under dark conditions of NO_2 and H_2O yielding HONO as well as a three body reaction leading to the formation of HONO with NO, NO_2 and H_2O participating, though the HONO production seems to be mostly depended on NO_2 and water concentrations and not as much in the presence of NO.~~ Svensson et al., 1987; ~~studied the kinetics of the NO_2 and water reaction deriving a rate for the~~

~~decay of NO_2 related to the surface to volume ratio of the reactor used.~~ Jenkin et al., 1987). ~~did not see a significant change of the previous reaction in respect to mild temperature variations.~~

Akimoto et al.~~,~~ (1987) and Sakamaki and Akimoto (1988) reported higher~~found~~ ~~that~~ HONO concentrations at higher light intensity. Auxiliary mechanisms ~~are enhanced from light yielding an extra source of OH radicals. Glasson and Dunker, 1989 proposed a kinetic mechanism based on the CO/NO_x measurements under Xe lamp illumination. Besides HONO, other OH sources such as nitric acid, the photolysis of O_3,formaldehyde and the reaction of O_3 with alkenes,have also been identified(Killus and Whitten, 1990; Finlayson-Pitts et al., 2003). Proposed auxiliary mechanisms~~ have been developed to describe the ~~for the chamber~~ background reactivity of smog chambers ~~in several facilities~~ (Bloss et al., 2005; Carter et al., 2005; Hynes et al., 2005; Rohrer et al., 2005; Metzger et al., 2008~~;~~ Wang et al., 2011; Wang et al., 2014). In these ~~mechanisms~~mechanisms, the role of the chamber walls as sinks and sources of gas-phase pollutants is parameterized and these reactions are added to the actual gas-phase chemistry model used to interpret the measurements in the chamber.~~effects of O_3 decay due to the walls as well as the OH formation due to off-gassing of HONO and other speciesis parameterized.~~

Typically, smog chamber experiments isolate a pollutant or a mixture of pollutants emitted by a source and focus on its chemistry. In most cases, clean air is used as the starting point of the experiment. While the corresponding results are clearly valuable, these experiments might miss the potentially important interactions of the examined chemical system with other pollutants existing in ambient air. To close this major gap between the laboratory studies and the ambient atmosphere, a portable dual smog chamber system with UV lights is designed and tested in this study. The chamber has been developed to use ambient air rather than clean air as its starting point. Having the advantage of being portable enhances the opportunities to study several environmental scenarios and simulate the processes occurring in previously out-of-reach chemical regimes (e.g., very aged air masses). The preliminary tests of the operation of this system are presented.

2. Design of the dual smog chamber system

2.1 Smog chambers

Relatively small Teflon reactors were selected for this system so that they can be filled in a matter of minutes, while having a volume adequate to support a 4-hourbatch experiment, losing less than a third of their volume based on the standard instrumentation sampling flow rates. A set of two identical smog chambers was constructed from Teflon (PTFE) ~~0.2 μm~~ film (~~Dupond~~DuPont PTFE 2 mil, 0.5 m wide.). Each chamber has a nominal volume of 1.5 m^3. The two chambers are pillow-shaped and are permanently mounted on a metal frames (Figure 1a). The relatively small volume of the chambers along with the fixed frame enables their easy and safe transport without having to disassemble them or to remove the sampling ports. Relative humidity (RH) and temperature sensors are also fixed on the chambers. The frame dimensions are 1.7 x 0.5 x 1.7 m. Two sampling ports (one per chamber) with multiple lines and a temperature-/-RH sensor were installed on the reactors.

We constructed the chambers ~~The chambers were built by us~~ in our laboratory in Patras. The reactors ~~Greece and~~ were thoroughly cleaned and conditioned before the first characterization experiment~~s~~. The~~ir~~ cleaning procedure involved first ~~passing~~ introduction of high O_3 concentrations with the UV lights on and heating to approximately 50 ^oC. Clean air was passed then through chambers for several hours. ~~A blank experiment was performed every few experiments~~ Blank experiments were performed periodically both in the lab (during the characterization phase) and in the field. The particle wall losses are measured ~~in~~ after each field experiment. We did not observe any evolution of the wall chemical behavior in these initial tests. ~~, but it something that we will keep investigating in future work.We did our best to clean the walls after the construction of the chambers from any residue of the Teflon production process but some volatile or semivolatile material could be still in theory present.~~

Sampling is alternated between the two chambers every three minutes by an automated three-way valve synchronized with the operation of the corresponding instrumentation. This allows a total duration of the experiments of more than 4 hours without the addition of make-up air. In order to eliminate interferences and memory effects due to this periodical alteration of the sampling lines, adequate time (30 s) is allowed within the three-minute sampling cycle for the lines to be flushed with the sample air from the next chamber. This is achieved by synchronizing the line flushing with the measuring instrumentation and discarding the data collected during this 30 s period.

2.2 Portable UV lighting system

A hemispheric design was selected with sixty 36 W UV light lamps (Osram, L36W/73) in a hexagonal arrangement. The lamps were mounted on five metal frames (12 per frame) creating five sub-structures (Figure 1b) that can be easily disassembled and transported. Once assembled the UV light support structure had a footprint of 4.5 x 4.5 m and a height of 2.5 m. Figure 1b shows the UV light assembly without the covering material. Flexible tent poles were used to create a dome that can be partially or fully covered protecting the chambers from the weather elements (Figures 1c and 1d). The sixth side does not include lights and is used as an entrance for chamber maintenance. The lights can be remotely operated at 20, 40, 60, 80 and 100% levels. The light fixtures include aluminum mirrors in order to direct the light towards the center of the dome, thus maximizing the light intensity delivered to the chambers. When all lights are on, the corresponding J_{NO2} is 0.1 min^{-1}. The spectrum of the lights~~lamps~~ peaks in the 350-400 nm region (SI Figure S1). The two chambers are placed inside this dome having at least a 0.5 m clearance from the UV lights when full. This design also allows the use of a single 10 m^3 chamber if so desired.

2.3 Subsystems

A dual-head metal bellows pump (model MB-602) is used to fill the chambers with ambient air delivering 80 L min^{-1} per pump head. Both chambers can be filled in around 20 min~~utes~~. Manual two-way valves were installed prior to the chamber inlets for isolation and selective filling purposes. Prior to any experiment with ambient air, both chambers are flushed with ambient air with the metal bellows pump until the NO_x and O_3 levels matched the ambient concentrations. To ensure chamber similarity the chambers are used alternatively in experiments as a perturbation/reference chamber.

If required clean particle free air can be introduced in the chambers. Dry air is generated by an oil-less compressor (Bambi VT200D) and further purified by activated carbon (Carbon cap, Whatman), HEPA filters (HEPA capsule, Pall) and silica gel (Silica gel rubin, Sigma-Aldrich). The compressor and air cleaning system ~~is~~are not used for the actual experiments. In these experiments the chambers are filled with ambient air without the use of cleaning devices. The compressor/cleaning system is used for the cleaning of the chambers between experiments and for blank or other chamber characterization experiments. Typically, the concentrations of

ozone, NO_x and larger VOCs ~~values~~ ~~,~~are below or close to the detection limit in the chambers when they are filled with clean air from our system. The scrubbers were replaced regularly and the residence time inside them was kept as high as possible (maintaining the corresponding flow rates as low as possible). The concentrations of some of the small oxygenated VOCs such as acetone, acetic acid and methanol were slightly elevated compared to the cylinder zero air.

A subunit including the above systems (except for the filling pump and the compressor) was added to one of the metal frames of the system. This subunit also includes a syringe pump, an atomizer (TSI model 3076) and a silica gel diffusion drier (Silica gel rubin, Sigma-Aldrich) for seed generation. Additionally, a bubbler subsystem for HONO introduction and an ozone generator (Azcozon, model HTU-500) were used. The concentration of OH when HONO was added was estimated in all experiments by the decay of d-butanol over time. The estimated levels of added HONO we~~added a~~re of the order of 100 ppb. Two temperature/RH sensors (Omega, model RH-usb) and a personal computer with Labview control for the sampling selection valve are also part of this system.

2.4 Instrumentation

The set of instruments selected for the use with the chamber system include: aHR-ToF-AMS (Aerodyne Research Inc.), a PTR-MS (Ionicon Analytik), a Scanning Mobility Particle Sizer (SMPS, classifier model 3080, DMA model 3081, CPC model 3787, TSI), an ozone monitor (API Teledyne, model 400E) and a NO_x monitor (API Teledyne, model T201). These instruments are located inside the FORTH mobile laboratory (Fig 1c) next to the chambers. Details on the instrumentation used can be found elsewhere (Kostenidou et al., 2013; Kaltsonoudis et al., 2016~~, Florou et al., 2018~~). With this configuration, a total sampling flow rate of 2.5-3 L min^{-1} is used that removes less than 0.1 m^3 ~~-~~from each chamber per hour.

2.5 Experimental procedure

The instrumentation is first used to characterize the ambient conditions for at least a couple of hours. After filling of the chambers is completed, sampling is switched from ambient measurements to the chambers and an initial characterization of the sampled air inside the chambers takes place. Then a perturbation (addition of oxidant or pollutant) is implemented in

one of the chambers, while the other is used as a reference. Following the completion of the experiment ammonium sulfate seeds are introduced into both chambers to measure their loss rate on the walls over time. In this step, the chambers may be refilled with particle free air. This last stage is used to quantify the particle size-dependent wall loss rate constants in order to make corrections to the rest of the measurements. Finally, the instrumentation is switched back to ambient observations and the chambers are flushed with either ambient air and /or clean air in preparation for the next experiment.

3. System evaluation

The system was developed and evaluated in Patras, Greece and also during the Finokalia Aerosol Measurement Experiment (FAME 16) campaign. Finokalia is a remote site in Crete, Greece (Kouvarakis et al., 2000). The field campaign took place during May-June 2016. Additional tests aimed on improving the performance of the setup were performed indoors at Carnegie Mellon University in Pittsburgh, United States. ~~The paper is based on the results of~~The present work is based on the results of 51 chamber characterization experiments and 7 field test experiments. The characterization experiments include 15 blank or contamination related experiments, 14 experiments characterizing wall losses, 6 experiments quantifying the ambient air sampling efficiency, 3 experiments for the measurement of J_{NO2}, 9 experiments related to RH and UV variations, and 4 VOC loss experiments. The list of these experiments and some additional information can be found in Table S1 in ~~details of these experiments has been added to~~ the Supplementary Information ~~(Table S1)~~.

3.1 Contamination tests

Tests were conducted in the field in order to assess the potential contamination of the chambers by ambient air. The chambers were filled with clean (particle free) air and the particle concentration inside the chambers was monitored by an SMPS. Figure 2 shows the total number concentrations in the two chambers. The particle number concentrations remained below 10 cm^{-3} in both chambers for several hours. The aerosol mass concentration (not shown) was less than 0.01 μg m^{-3}. This suggests that clean conditions can be maintained for both chambers for the duration of a typical field experiment.

3.2 Chamber similarity

Similar results should be obtained when identical experiments take place in the two chambers in order to safely use one of them as reference. To establish this, ambient air was introduced in both chambers and the evolution of the concentrations and composition of the particulate matter and gas pollutants was measured. An SMPS measured the size distribution and an AMS the particulate composition. The measured chamber and ambient mass concentrations (Figure 3a) and the AMS spectra (Figures3c and d) were in good agreement between the two chambers and the ambient. The particle mass concentration in the chambers was approximately 85% of the ambient levels. The theta angle (Kostenidou et al., 2009) between the organic aerosol spectra in the two chambers and the ambient air was in the range of 2.5-6 degrees, suggesting that identical results can be obtained when filling these chambers with ambient air and that the filling process does not contaminate the air sample. The theta angle is a measure of the similarity of the OA spectra (similar to the often used R^2). E~~It treats e~~ach mass spectrum is treated as a vector (each *m/z* is an element of the vector) and ~~expresses~~theta is the angle between two such vectors~~spectra~~. We prefer to use theta angle for AMS spectra comparisons because it can distinguish better small differences in spectra that the coefficient of determination cannot.

Pump and tubing losses during the filling procedure were evaluated in order to establish the difference between ambient concentrations and the ones obtained in the chambers. The same number distributions are achieved in both chambers after filling them with ambient air. The penetration efficiency through the tubing and the pump for particles with diameter larger than 80nm is close to 100%, while for smaller particles due to higher diffusional deposition the penetration efficiency is 45%. The length of the tubing is approximately one meter (with a 0.5 -in~~ch~~ diameter). The estimated losses for this tube for the flow rates used and for particles in the 20-80 nm size range are 1-3 percent. Therefore, most of the losses are ~~indeed due to~~~~occuring~~occurring in the pump.

3.3 Particle wall losses

Loss of particles to the walls is one of the processes that complicate the analysis of smog chamber experiments. The use of smaller reactors with lower surface to volume ratios can accelerate these losses. Disturbances of the Teflon reactors tend to increase the wall loss rates

due to the buildup of static charges on the chamber walls. Transporting and installing the reactors also results in higher wall loss rate constants (Wang et al., 2018).

In order to assess the wall loss behavior of the system experiments were conducted both in the laboratory and in the field. In all cases, ammonium sulfate seeds were added to the chambers and their decay with time was measured. Typically, the chambers were first filled with clean (particle free) air and then ammonium sulfate seeds were introduced. A solution of 5 g L^{-1} ammonium sulfate was used for the atomizer and a flow rate of 2 L min^{-1}. The decay of the particles was monitored by an SMPS. Size dependent wall loss rate constants were calculated correcting for coagulation (Wang et al., 2018). Figure 4a represents the average size dependent profiles for the loss rate constant K_c of the two chambers for the laboratory experiments. On the field, higher rate loss constants were measured (Figure 4b). For example, loss rate constants of 0.2 h^{-1} were measured for the 350 nm particles in the lab, while for the same size range, a value of approximately 0.5 h^{-1} was measured in the field. Figure 4c and 4d show the wall loss profiles of the two chambers when deployed in the Finokalia campaign over three days of measurements. In both chambers the wall loss rate constants were decreasing over time. During the field deployment of the chambers their handling and the corresponding induced friction ~~of the walls and thehandling~~ resulted in higher charges on the chambers walls and thus~~s resulting in~~ higher particle wall losses. These higher losses had also a stronger size dependence. On the other hand, when the chambers were inside the lab, there was no build-up of charges and the losses were lower and less size-dependent. ~~We have recently presented a~~A detailed analysis of the losses of particles in ~~our~~ Teflon chambers (both in the laboratory and the field~~ ones~~) has been~~was~~ presented by~~in~~ Wang et al. (2018). ~~where wall loss rates increase after a disturbance (eg. service off the chamber) and take a considerable amount of time to achieve the conditions prior to the disturbance.~~

~~———~~For this reason, the particle wall loss rates are measured after each experiment, by the addition of ammonium sulfate seeds~~ as a final step~~. The chambers in the laboratory underwent minimum handling during each experiment and thus achieved low loss rate constants for a wide range of particle sizes. ~~The chambers deployed in the field had higher particle wall loss rate constants, due to higher static charges on them. The static charge originated from the transportation and handling of the chambers.~~

In order to assess if it is possible to minimize such charges a test was conducted in the Teflon reactors in the lab. The chambers were moved in a different location inside the building where the lab is located. The two reactors were handled in exactly the same way simulating the handling during a field deployment. One of the chambers was inflated with air to almost half-full while the other was empty. The particle wall-losses were measured before and after the movement. Figure 5 represents the loss rate constants in the two chambers because of the movement. The loss rate did not change in the partially inflated chamber. The other chamber though experienced an increase in the loss rate constants, almost doubling for the particles in the range 50-200 nm, due to stronger friction of the Teflon walls with each other and thus building static charge. No significant change was noticed for particle larger than 250 nm.

The high particle wall losses introduce uncertainty in the results, because the wall-loss corrections dominate the corrected concentration values. If the losses are very high, the maximum duration of such experiments may be limited. We have been working on developing methods to minimize these effects. Moving the chambers to the field site either fully or at least partially inflated inside our mobile laboratory clearly helps. ~~We have also been exploring other means of reducing these surface changes in the field.~~

3.4 VOC concentrations

Concentrations of the VOCs measured by the PTR-MS were within a few percent of their ambient levels. In most cases, no noticeable differences were seen. Tests indicated that there was no detectable contamination due to the metal bellows pump during the filling process of the two chambers. ~~We have performed vapor loss experiments for a few selected VOCs~~Vapor loss experiments were also performed for a few selected VOCs. The measured wall loss rates were quite low (less than 1 percent per hour) ~~in respect to~~for toluene and a-pinene. Their concentrations remained for all practical purposes stable ~~for at least three hours per Experiment~~during the experiment.

3.5 ~~Nitrogen oxides, ozone, light and nitrous acid characterization~~NO_x, O_3, and OH interactions with the walls

A series of e~~E~~xperiments were performed to quantify the loss rates of NO_x and O_3 to the Teflon walls of the chambers and the OH production rates. These can be used for the development of an

auxiliary mechanism. ~~related to the fate of nitrogen oxides, ozone and nitrous acid in respect to the Teflon walls were performed and a basic auxiliary mechanism is proposed (SI).~~ The experiments were carried out for~~under~~ two ~~different~~ light intensities (J_{NO2} of 0.03 min^{-1} and 0.1 min^{-1}) and for ~~under~~ two ~~different~~ RH values (RH<10% and ~~RH=~~50-±-15%). The OH levels in the chamber were estimated based on the decay of d-butanol. HONO off-~~-~~gassing from the chamber walls was not measured directly, but was estimated based on the OH levels~~blank experiments under the different conditions UV and RH conditions discribeddescribed above. The chamber HONO concentration was measured HONO's estimation was done based on the decay of d-butanol when the UV lights were turned 'ON'on.~~. Effective OH production rates were estimated using a pseudo-steady-state assumption.

~~For the HONO off-gassing, if we assumeassuming a pseudo-steady state for the OH radicals we can estimate theireffective production rate.~~ The OH production rates were~~is~~ practically negligible at low RH, but ~~it did~~ increased at 50 ~~percen~~% RH~~t%~~ and depended on light intensity. The results of these measurements can be found in the SI. These measurements indicate that the HONO injections were the ~~-~~dominant source of OH in our perturbation experiments. However, the contribution of the walls can be non-negligible under some conditions for the baseline chamber. To minimize complications, ~~OH producedduring the simulation experiments with ambient air,was from our HONO injections and not theOH due to the walls. This is the dominant source of OH in our perturbation experiments.One important note for our experiments is that~~B~~ because~~ d-butanol~~ is~~ was injected in all ~~ofthem~~ experiments allowing the direct estimation of ~~,~~ the OH concentration in both chambers. As a result ~~is estimated directly and therefore the~~ the reported OH exposure ~~reported is alreadytaking~~takes into account the wall sources as well.

4. Laboratory testing

The performance of the system was ~~in use~~ tested in experiments that took place indoors at Carnegie Mellon University (Center for Atmospheric Particle Studies~~—CAPS~~). The potential aging of urban background air masses in Pittsburgh, PA, by OH radicals was used as a pilot study for the system evaluation. Fewer UV lights were used in this test resulting in a J_{NO2} equal to 0.03 min^{-1}.

4.1 Experimental procedure

Prior to the experiment, both chambers were flushed with particle-free air overnight under UV illumination to remove any residual particles and gas-phase organics. Both chambers were filled with ambient air using the metal bellows pump. During the filling procedure, the instruments were measuring ambient conditions. After the addition of ambient air in the chambers, d9-butanol (60 ppb) was added to both of them as an OH tracer (Barment et al., 2012). The OH levels can be estimated by the decay in the d9-butanol concentration measured be the PTR-MS system at *m*/*z* 66. The reaction constant for the butanol reaction with OH is 3.4 x 10^{12} cm^3 $molecules^{-1}$ s^{-1}. HONO was injected only into the perturbation chamber for about 3 min to produce OH upon UV illumination. The UV lights then turned on were illuminating both chambers. After the completion of the perturbation experiment, a seed wall-loss experiment was conducted to quantify the particle wall-loss rate constants for the two chambers as described in section 3.3.

4.2 Results and discussion

The wall-loss corrected total particle number concentration as measured by the SMPS ~~are~~ is shown in Figure 6. The instruments were measuring ambient conditions during the filling process. The average ambient number concentration was around 2500 cm^{-3}. HONO was injected in the perturbed chamber at *t*=0.4 h. After turning on the UV lights (*t*=0.6 h) an increase in the total particle number and volume in the perturbed chamber was observed while no change in the control chamber was noticed. The increase in the perturbed chamber is due to the formation of new particles (Figure 7).

Based on the AMS measurements, the ambient air used to fill the chambers contained on average 3.6 μg m^{-3} of non-refractory PM_1 with organics accounting for 75%, sulfate 17%, ammonium 6% and nitrate 2%. The collection efficiency of the AMS measurements was found to be 0.6 based on the algorithm of Kostenidou et al. (2007), while the estimated OA density was 1.2 g cm^{-3}. The calculated theta angle (Kostenidou et al., 2009) between the ambient and the chamber organic mass spectra vectors was around 5 degrees, indicating that the aerosol composition inside the chamber was essentially the same as in the ambient.

To quantify the secondary aerosol formation, data were corrected for both the collection efficiency and for particle wall-losses. Figure 8 shows the concentrations of the major PM_1

components in the two chambers. An increase of concentration was observed in the perturbed chamber. After 2.5 hours of exposure to OH an additional 1.5 μg m^{-3} of organics, 0.2 μg m^{-3} of sulfates, 0.1 μg m^{-3} of nitrates and 0.1 μg m^{-3} of ammonium was formed. The average OH concentration in the perturbed chambers was 8.0×10^6 molecules cm^{-3} corresponding to approximately 11 h of equivalent exposure to an ambient OH=1.5×10^6 molecules cm^{-3}. The OH concentration in the control chamber was an order of magnitude less 8×10^5 molecules cm^{-3}. The organic spectra of the additional formed SOA and the initial OA in the perturbed chamber were relatively similar; their theta angle was 10 degrees (Figure 9). The mass spectrum of the processed OA characterized by lower fractional contributions at *m*/*z* 43 and 44.

The evolution of the oxygen to carbon ratio of the organic aerosol in the two chambers is shown in Figure 10. The O:C of the ambient organic aerosol and of the initial OA in the two chambers was 0.44. After the OH introduction and the SOA production in the perturbed chamber, the O:C decreased slightly to 0.40. The O:C in the control chamber remained approximately the same. The decrease of the O:C in the perturbed chamber indicates that the additional formed SOA had smaller O:C than the ambient. The average O:C ratio in other ambient experiments conducted in Pittsburgh was around 0.5 indicating an already moderately oxidized aerosol population. For comparison, the average O:C ratio in the FAME 2008 and FAME 2009 campaigns was 0.8 and 0.5, respectively (Hildebrandt et al., 2010). The results of ~~several~~ such ambient air experiments with detailed analysis of the formed aerosol, comparison with ambient and laboratory measurements are included in a forthcoming publication.

5. Conclusions

A portable dual chamber system has been developed for field studies using ambient air as a starting point. The system has been evaluated and no contamination was observed during a typical experiment. The concentration in the two chambers when filled with ambient air are within a few percent of each other. Particle losses during filling were less than 20%. No noticeable losses or cross-contamination was observed for the measured VOC species.

Higher wall loss rates were observed when the chambers were deployed in the field, compared to the lower and stable rates observed when the chambers were inside the laboratory, due to higher electrostatic charges induced during their movement. A reduction in the wall loss

rates was observed when the chambers are deployed in the field, suggesting that they should be measured after each experiment. The losses can be reduced if the chambers are transported partially inflated. Initial laboratory experiments show promising results in respect to potential aging properties of urban background air in Pittsburgh. An additional 1.5 μg m^{-3} of SOA was formed after 12 h of equivalent OH exposure with a moderate decrease of the O:C ratio. Implementing the system in the field will enable the study of complex systems that were previously out of reach with traditional stationary chamber facilities.

Data availability. The data in the study are available from the authors upon request (spyros@chemeng.upatras.gr).

Author contributions. CK constructed the facility, participated in the experiments and wrote the paper. SJ conducted and~~,~~ analysed the wall loss and test experiments and contributed to the writing of the paper. EL and KF helped in the construction of the facility and assisted in the experiments. SNP was responsible for the design of the study, the synthesis of the results and contributed to the writing of the paper.

Competing interests. The authors declare that they have no conflict of interest.

*Acknowledgements.*This research was supported by the European Research Council Project ATMOPACS (Atmospheric Organic Particulate Matter, Air Quality and Climate Change Studies) (Grant Agreement 267099). This work has also received funding from the European Union's Horizon 2020 research and innovation program~~me~~ through the EUROCHAMP-2020 Infrastructure Activity under grant agreement No 730997.

References

Akimoto, H., Hishino, M., Inoue, G., Sakaaki, F., Washida, N. and Okuda, M.: Design and characterization of the evacuable and bankable photochemical smog chamber, Environ. Sci. Technol., 13, 471–475, 1979.

Akimoto, H., Takagi, H. and Sakamaki, F.: Photo enhancement of nitrous acid formation in the surface reaction of nitrogen dioxide and water vapor: Extra radicals source in smog chamber experiments. Inter. J~~our~~. ~~of~~ Chem. Kinetics, 19, 539-551, 1987.

Barmet, P., Dommern, J., DeCarlo, P.F., Tritscher, T., Praplan, A.P., Platt, S.M., and Prevot, A.S.H.: OH clock determination by proton transfer reaction mass spectrometry at an environmental chamber. Atmos. Meas. Tech., 5, 647–656, 2012.

Bloss, C., Wagner, V., Bonzanini, A., Jenkin, M. E., Wirtz, K., Martin-Reviejo, M., and Pilling, M. J.: Evaluation of detailed aromatic mechanisms (MCMv3 and MCMv3.1) against environmental chamber data, Atmos. Chem. Phys., 5, 623-639, 2005.

Carter, W. P.L., Atkinson, R., Winer, A.M. and Pitts, J.N. JR.: Experimental investigation of chamber dependent radical sources. Inter. J~~our~~. ~~of~~ Chem. Kinetics, 14, 1071-1103, 1982.

Carter, W.P.L., Cocker, D.R., Fitz, D.R., Malkina, I.L., Bumiller, K., Sauer, C.G., Pisano, J.T., Bufalino, C., and Song, C.: A new environmental chamber for evaluation of gas-phase chemical mechanisms and secondary aerosol formation, Atmos. Environ., 39, 7768–7788, 2005.

Cocker D. R., Clegg, S. L., Flagan, R. C., and Seinfeld, J. H.: The effect of water on gas–particle partitioning of secondary organic aerosol. Part I: a-pinene/ozone system. Atmos. Environ., 35, 6049–6072, 2001b.

Cocker, D. R., Flagan, R.C., and Seinfeld, J. H.: State-of-the-art chamber facility for studying atmospheric aerosol chemistry, Environ. Sci. Technol., 35, 2594-2601, 2001a.

Finlayson, B., Pitts, J. N.: Photochemistry of the polluted troposphere. Science, 192, 111-119, 1976.

Finlayson-Pitts, B.J., –Wingen, L.M., Summer, A.L., Syomin, D. and Ramazan, K.A.: The heterogeneous hydrolysis of NO_2 in laboratory systems and in outdoor and indoor atmospheres: An integrated mechanism. Phys. Chem. Chem. Phys., 5, 223-242, 2003.

Glasson, W. A. and Dunker, A. M.: Investigation of background radical sources in Teflon-film irradiation chamber. Environ. Sci. Technol., 23, 970-978, 1989.

Hallquist, M., Wenger, J. C., Baltensperger, U., Rudich, Y., Simpson, D., Claeys, M., Dommen, J., Donahue, N. M., George, C., Goldstein, A. H., Hamilton, J. F., Herrmann, H., Hoffmann, T., Iinuma, Y., Jang, M., Jenkin, M. E., Jimenez, J. L., Kiendler-Scharr, A., Maenhaut, W., McFiggans, G., Mentel, T. F., Monod, A., Prevot, A. S. H., Seinfeld, J.

H., Surratt, J. D., Szmigielski, R. and Wildt, J.: The formation, properties and impact of secondary organic aerosol: current and emerging issues. Atmos. Chem. Phys., 9, 5155–5236, 2009.

Heisler, S.L., and Friedlander, S.K.: Gas to particle conversion in photochemical smog: Aerosol growth laws and mechanisms for organics, Atmos. Environ., 11, 157-168, 1977.

Hennigan, C. J., Miracolo, M. A., Engelhart, G. J., May, A. A., Presto, A. A., Lee, T., Sullivan, A. P., McMeeking, G. R., Coe, H., Wold, C.E., Hao, W. M., Gilman, J. B., Kuster, W. C., deGouw, J., Schichtel, B. A., Collett Jr., J. L., Kreidenweis, S. M., and Robinson, A. L.~~\~~: Chemical and physical transformations of organic aerosol from the photo-oxidation of open biomass burning emissions in an environmental chamber, Atmos. Chem. Phys., 11, 7669–7686, 2011.

Hildebrandt, L., E. Kostenidou, N. Mihalopoulos, D.R. Worsnop, N.M. Donahue, and S. N. Pandis (2010), Formation of highly oxygenated organic aerosol in the atmo-sphere: Insights from the Finokalia Aerosol Measurement Experi-ments, Geophys. Res. Lett.,37, L23801, doi:10.1029/2010GL045193.

Hoffmann, T., Odum, J. R., Bowman, F., Collins, D., Klockow, D., Flagan, R. C., and Seinfeld, J. H.: Formation of organic aerosols from the oxidation of biogenic hydrocarbons. J. Atmos. Chem. 26, 189–222, 1997.

Hynes, R.G., Angove, D.E., Saunders, S.M., Haverd,V. and Azzi, M.: Evaluation of two MCM v3.1 alkene mechanisms using indoor environmental chamber data, Atmos. Env., 39, 7251-7262, 2005.

Jeffries, H., Fox, D., and Kamens, R.: Outdoor smog chamber studies: light effects relative to indoor chambers, Environ. Sci. Technol., 10, 1006-1011, 1976.

Jenkin, M. E., Cox, R. A. and Williams, D. J.: Laboratory studies of the kinetics of formation of nitrous acid from the thermal reaction of nitrogen dioxide and water vapor. Atmos. Env ~~Env~~. 22, 487-498, 1988.

Kaltsonoudis, C., Kostenidou, E., Louvaris, E., Psichoudaki, M., Tsiligiannis, E., Florou, K., Liangou A., and Pandis, S.N.: Characterization of fresh and aged organic aerosol emissions from meat charbroiling, Atmos. Chem. Phys. 17, 7143–7155, 2017.

Kelly, N.A., and Gunst, R.F.: Response of ozone to changes in hydrocarbon and nitrogen oxide concentrations in outdoor smog chambers filled with Los Angeles air, Atmos. Environ., 24, 2991-3005, 1990.

Kelly, N.A.: The photochemical formation and fate of nitric acid in the metropolitan Detroit area: Ambient, captive-air irradiation and modeling results, Atmos. Environ., 21, 2163-2177, 1987.

Killus, J.P. and Whitten, G.Z.: Background reactivity in smog chambers. Inter. J~~our~~. ~~of~~ Chem. Kinetics, 22, 547-575, 1990.

Kim, Y.J., Platt, U., Gu, M.B., and Iwahashi, H.: Atmospheric and biological environmental monitoring, Springer, 2009.

Kleffmann, J., Becker, K.H. and Wiesen, P.: Heterogeneous NO_2 conversion processes on acid surfaces: Possible atmospheric implications. Atmos. Environ., 32, 2721-2729, 1998.

Kostenidou, E., Pathak, R.K., and Pandis, S. N.: An algorithm for the calculation of secondary organic aerosol density combining AMS and SMPS data, Aerosol Sci. Technol., 41, 1002–1010, 2007.

Kostenidou, E., Lee, B. H., Engelhart, G. J., Pierce, J. R., and Pandis, S. N.: Mass spectra deconvolution of low, medium and high volatility biogenic secondary organic aerosol, Environ. Sci. Technol., 43, 4884–4889, 2009.

Kostenidou, E., Kaltsonoudis, C., Tsiflikiotou, M., Louvaris, E., Russell, L. M. and Pandis, S. N.: Burning of olive tree branches: a major organic aerosol source in the Mediterranean. Atmos. Chem. Phys., 13, 8797–8811, 2013.

Kouvarakis, G., Tsigaridis, K., Kanakidou, M., and Mihalopoulos, N.: Temporal variations of surface background ozone over Crete island in the southeast Mediterranean, J. Geophys. Res., 105, 4399-4407, 2000.

Laity, J.: A smog chamber study comparing black light fluorescent lamps with natural sunlight, Environ Sci. Technol., 5, 1218-1220, 1971.

Lee, B.S., Bae, G.N., Moon, K.C., Choi, M.: Correlation between light Intensity and ozone formation for photochemical smog in urban air of Seoul, Aerosol Air Qual. Res., 10, 540-549, 2010.

Leone, J. A, Flagan, R.C., Grosjean, D. and Seinfeld, J.H.: An outdoor smog chamber and modeling study of toluene–NO_x photooxidation. Int. J. Chem. Kinetics, 17, 177–216, 1985.

Metzger, A., Dommen, J., Gaeggeler, K., Duplissy, J., Prevot, A. S. H., Kleffmann, J., Elshorbany, Y., Wisthaler, A., and Baltensperger, U.: Evaluation of 1,3,5 trimethylbenzene degradation in the detailed tropospheric chemistry mechanism, MCMv3.1, using environmental chamber data, Atmos. Chem. Phys., 8, 6453-6468, 2008.

Pathak, R. K., Stanier, C. O., Donahue, N. M., and Pandis, S. N.: Ozonolysis of alpha-pinene at atmospherically relevant concentrations: Temperature dependence of aerosol mass fractions (yields), J. Geophys. Res, 112, D03201, doi:10.1029/2006jd007436, 2007.

Paulsen, D., Dommen, J., Kalberer, M., Prevot, A.S.H., Richter R., Sax, M., Steinbacher, M., Weingartner, E., and Baltensperger, U.: Secondary organic aerosol formation by irradiation of 1,3,5-trimethylbenzene—-—NO_x-H_2O in a new reaction chamber for atmospheric chemistry and physics, Environ. Sci. Technol., 39, 2668-2678, 2005.

Pitts, J.N., Smith, J.P., Fitz, D.R., and Grosjean, D.: Enhancement of photochemical smog by N,N-diethylhydroxylamine in polluted ambient air, Science, 197, 255–257, 1977.

Pitts, J. N., Sanhueza, E.-, Atkinson, R., Carter, W. P.L., Winer, A. M., Harris, G. W. and Plum, C. N.: An investigation of nitrous acid in environmental chambers. Inter. J~~our~~. ~~of~~ Chem. Kinetics, 16, 919-939, 1984.

Platt, S. M., El-Haddad, I., Zardini, A. A., Clairotte, M., Astorga, C., Wolf, R., Slowik, J. G., Temime-Roussel, B., Marchand, N., Ježek, I., Drinovec, L., Močnik, G., Möhler, O., Richter, R., Barmet, P., Bianchi, F., Baltensperger, U., and Prévôt, A. S. H.: Secondary organic aerosol formation from gasoline vehicle emissions in a new mobile environmental reaction chamber. Atmos. Chem. Phys., 13, 9141-9158, 2013.

Roberts, P.T, and Friedlander, S.K.: Photochemical aerosol formation. SO_2, 1-heptene, and NO, in ambient air, Environ. Sci. Technol., 10, 573-580, 1976.

Rohrer, F., Bohn, B., Brauers, T., Brüning, D., Johnen, F.-J., Wahner, A., and Kleffmann, J.: Characterisation of the photolytic HONO-source in the atmosphere simulation chamber SAPHIR, Atmos. Chem. Phys., 5, 2189-2201, 2005.

Sakamaki, F., Hatakeyama, S. and Akimoto, H.: Formations of nitrous acid and nitric oxide in the heterogeneous reaction of nitrogen dioxide and water vapor in a smog chamber. Inter. Jour. of Chem. Kinetics, 15, 1013-1029, 1983.

Sakamaki. F. and Akimoto, H.: HONO formation as unknown radical source in photochemical smog chamber. Inter. Jour. of Chem. Kinetics, 20: 111-116, 1988.

Shibuya, K., and Nagashima, T.: Photochemical ozone formation in the irradiation of ambient air samples by using a mobile smog chamber, Environ. Sci. Technol., 6, 661-665, 1981.

Stockwell, C. E., Yokelson, R. J., Kreidenweis, S. M., Robinson, A. L., DeMott, P. J., Sullivan, R. C., Reardon, J., Ryan, K. C., Griffith, D. W. T., and Stevens, L.: Trace gas emissions from combustion of peat, crop residue, domestic biofuels, grasses, and other fuels: configuration and Fourier transform infrared (FTIR) component of the fourth fire lab at Missoula experiment (FLAME-4), Atmos. Chem. Phys., 14, 9727–9754, 2014.

Svensson, R., Ljungstrom, E. and Lindqvist, O.: Kinetics of the reaction between nitrogen dioxide and water. Atmos. Env. 21, 1529-1539, 1987.

Tritscher, T., Dommen, J., DeCarlo, P. F., Gysel, M., Barmet, P. B., Praplan, A. P., Weingartner, E., Prévôt, A. S. H., Riipinen, I., Donahue, N. M., and Baltensperger, U.: Volatility and hygroscopicity of aging secondary organic aerosol in a smog chamber. Atmos. Chem. Phys., 11, 11477-11496, 2011.

Tkacik, D. S., Lambe, A. T., Jathar, S., Li, X., Presto, A. A., Zhao, Y., Blake, D. R., Meinardi, S., Jayne, J. T., Croteau, P. L., and Robinson, A. L.: Secondary organic aerosol formation from in-use motor vehicle emissions using a potential aerosol mass reactor. Environ. Sci. Technol., 48, 11235–11242, 2014.

Ortega, A. M., Hayes, P. L., Peng, Z., Palm, B. B., Hu, W. W., Day, D. A., Li, R., Cubison, M. J., Brune, W. H., Graus, M., Warneke, C., and Gilman, J. B.: Real-time measurements of secondary organic aerosol formation and aging from ambient air in an oxidation flow reactor in the Los Angeles area. Atmos. Chem. Phys., 16, 7411–7433, 2016.

Wang, J., Doussin, J. F., Perrier, S., Perraudin, E., Katrib, Y., Pangui, E., and Picquet-Varrault, B.: Design of a new multi-phase experimental simulation chamber for atmospheric photosmog, aerosol and cloud chemistry research, Atmos. Meas. Tech., 4, 2465-2494, 2011.

Wang, X., Liu, T., Bernard, F., Ding, X., Wen, S., Zhang, Y., Zhang, Z., He, Q., Lu~~ü~~, S., Chen, J., Saunders, S., and Yu, J.: Design and characterization of a smog chamber for studying gas-phase chemical mechanisms and aerosol formation, Atmos. Meas. Tech., 7, 301-313, 2014.

Wang, N., Jorga, S. D., Pierce, J. R., Donahue, N. M., and Pandis, S. N.: Particle wall-loss correction methods in smog chamber experiments, Atmos. Meas. Tech.~~ Discuss.~~, 11, 6577–6588, 2018.~~doi:10.5194/amt-2018-175, 2018.~~

Warren, B., Song, C., and Cocker, D.R.: Light intensity and light source influence on secondary organic aerosol formation for the m-xylene/NOx photooxidation system, Environ. Sci. Technol., 42, 5461–5466, 2008.

Weitkamp, E. A., Sage, A. M., Pierce, J. R., Donahue, N. M., and Robinson, A. L.: Organic aerosol formation from photochemical oxidation of diesel exhaust in a smog chamber. Environ. Sci. Technol., 410, 6969–6975, 2007.

Figure 1. Pictures of the portable dual chamber system: a) the dual chambers; b) UV light assembly; c) field deployment during the FAME 16 study; d) system configuration with the UV lights on and the top cover open.

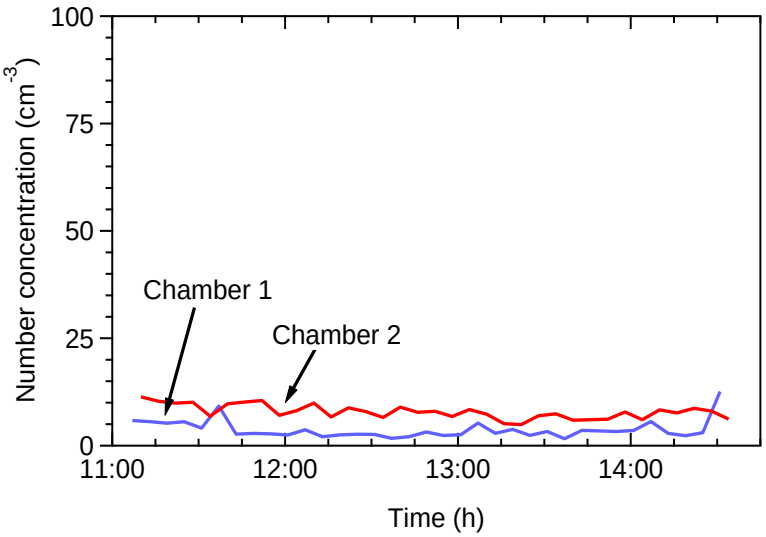

Figure 2. Total particle number concentrations as a function of time when the chambers were filled with clear air in the field for leak check of the chambers.

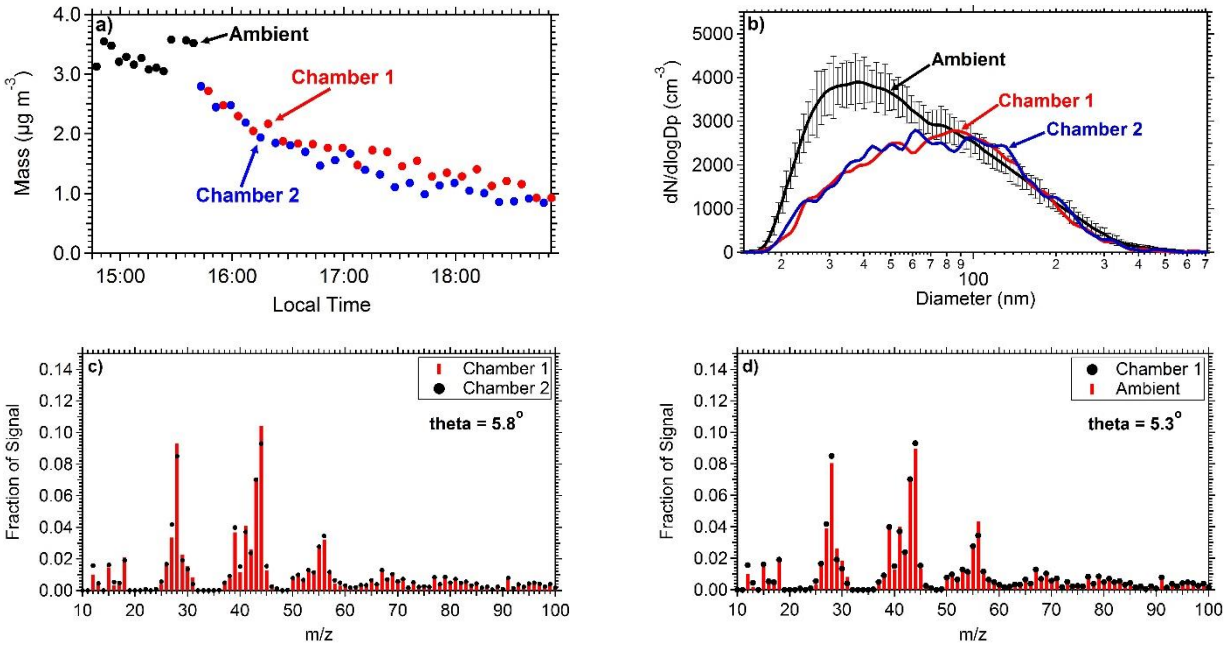

Figure 3. Comparison of the measurements between the two chambers and between ambient measurements: a) Mass concentration ($PM_{0.7}$) as measured by the SMPS in both the chambers and the ambient. b) Number distributions inside the chambers and in the ambient (the error bar represent one standard deviation). c) Average aerosol mass spectra of chamber 1 and chamber 2 filled with ambient air. d) Average aerosol mass spectra of ambient air and chamber 1.

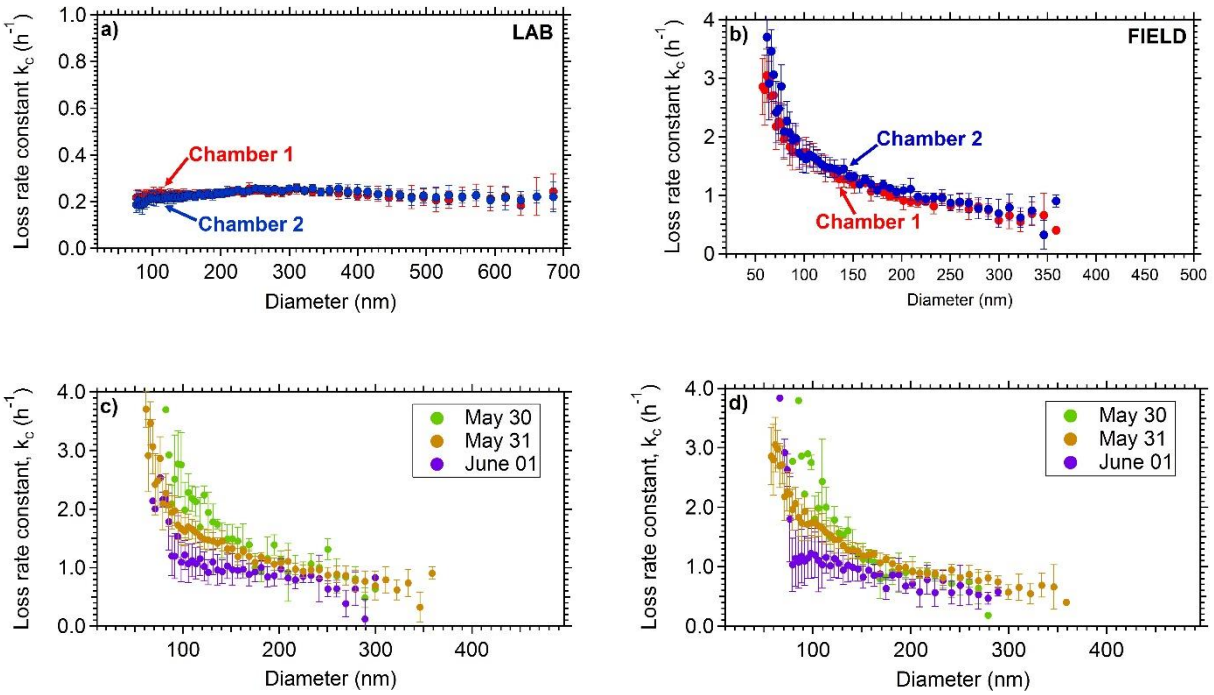

682 **Figure 4.** Coagulation-corrected particle wall-loss rate constant as a function of particle size for
683 the two chamber a) in the laboratory and b) in the field. The particle wall-loss rate constant as a
684 function of particle size during three consecutive days for the field deployment. Figure c
685 corresponds to chamber 1 and d) to chamber 2.
686
687
688
689
690
691
692

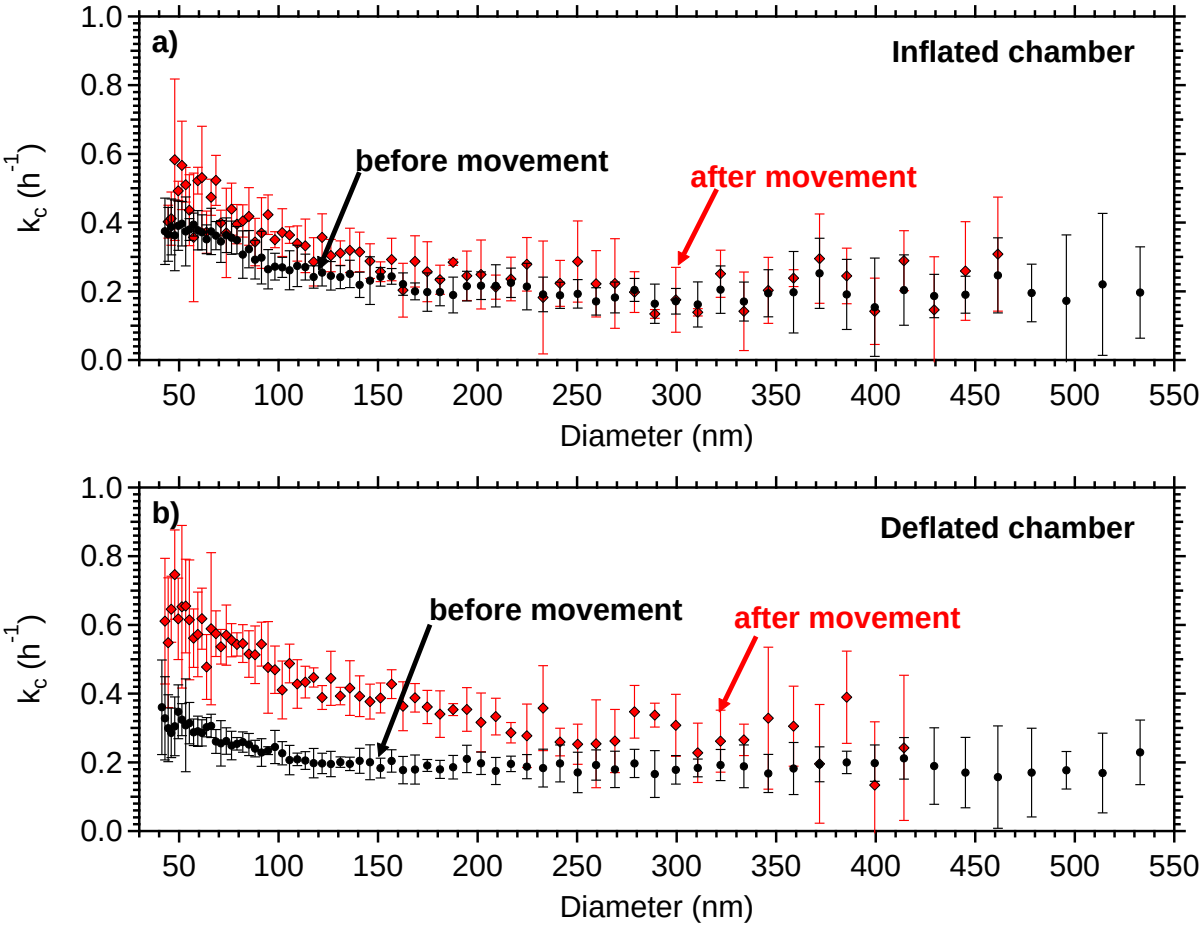

Figure 5. Coagulation-corrected particle wall-loss rate constant as a function of particle size for the two chamber after the movement a) in the partially inflated chamber and b) in the deflated chamber. The error bars represent one standard deviation.

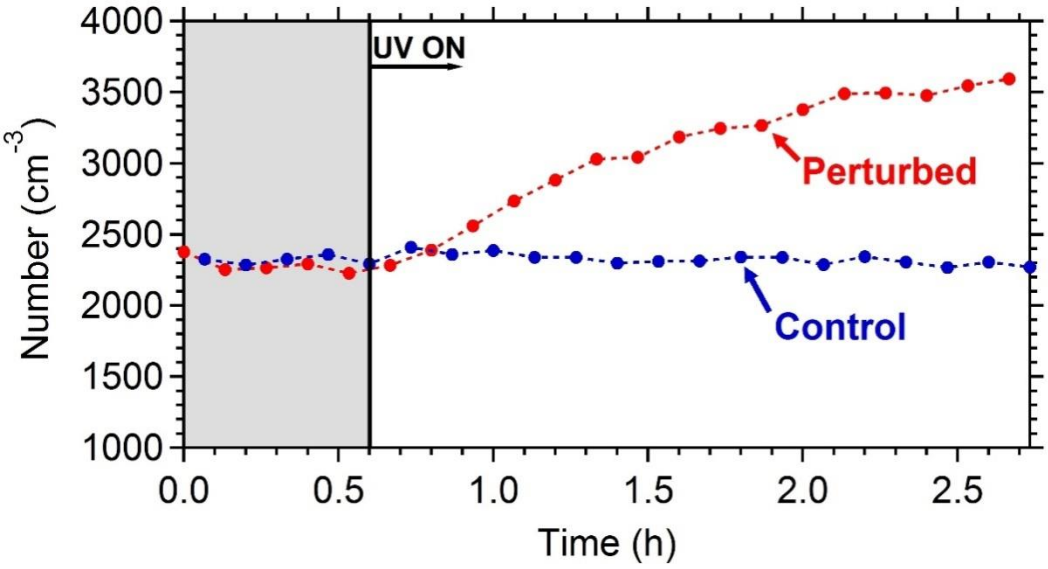

Figure 6. The wall-loss corrected SMPS-measured aerosol number concentration. HONO was added only in the perturbed chamber at t=–0.4 h to produce OH under UV illumination. The shaded area indicates that the chambers were dark.

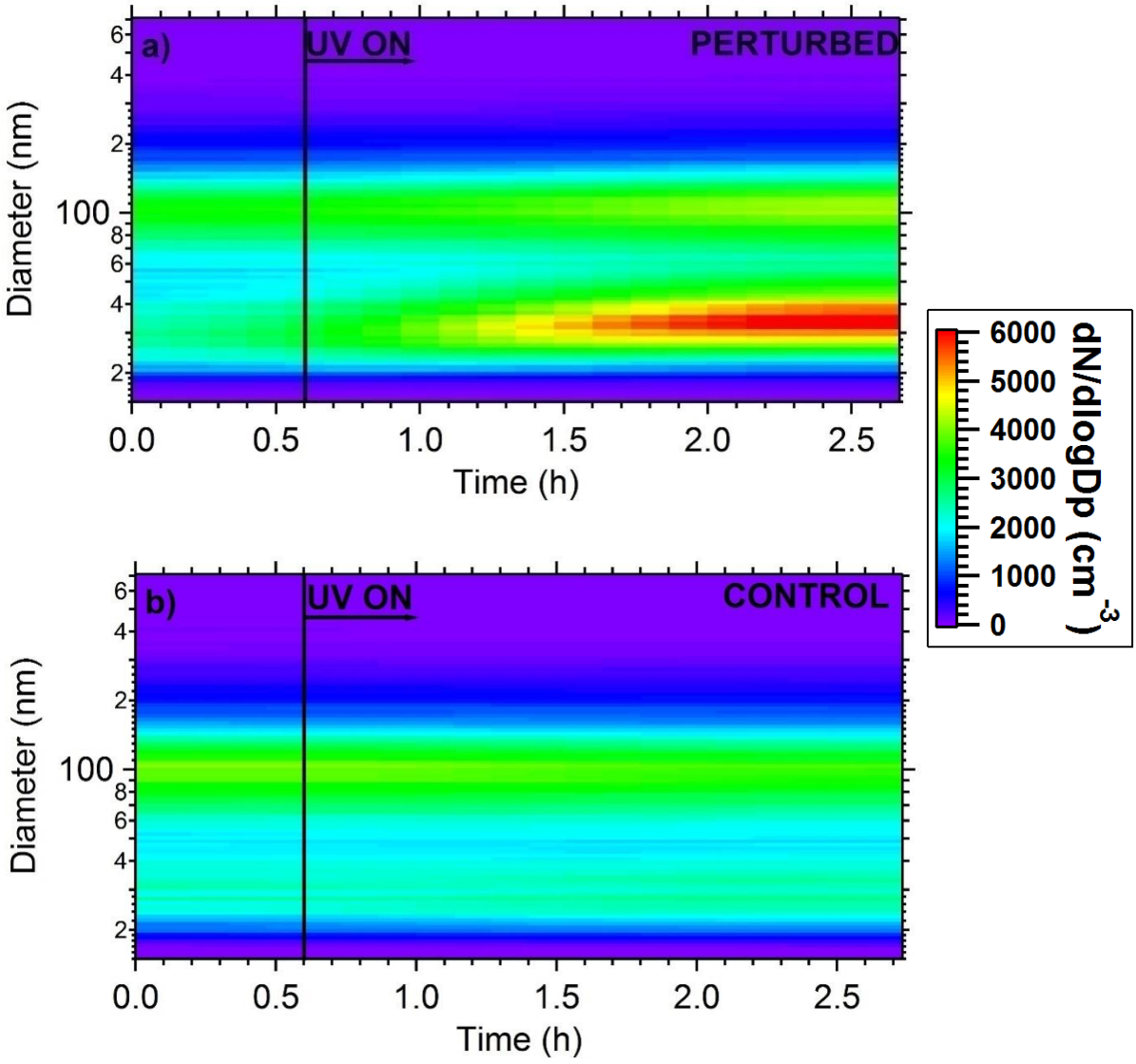

Figure 7. Plots of the evolution of particle number distributions during the HONO perturbation experiment in Pittsburgh. (a) Perturbed chamber and (b) Control chamber.

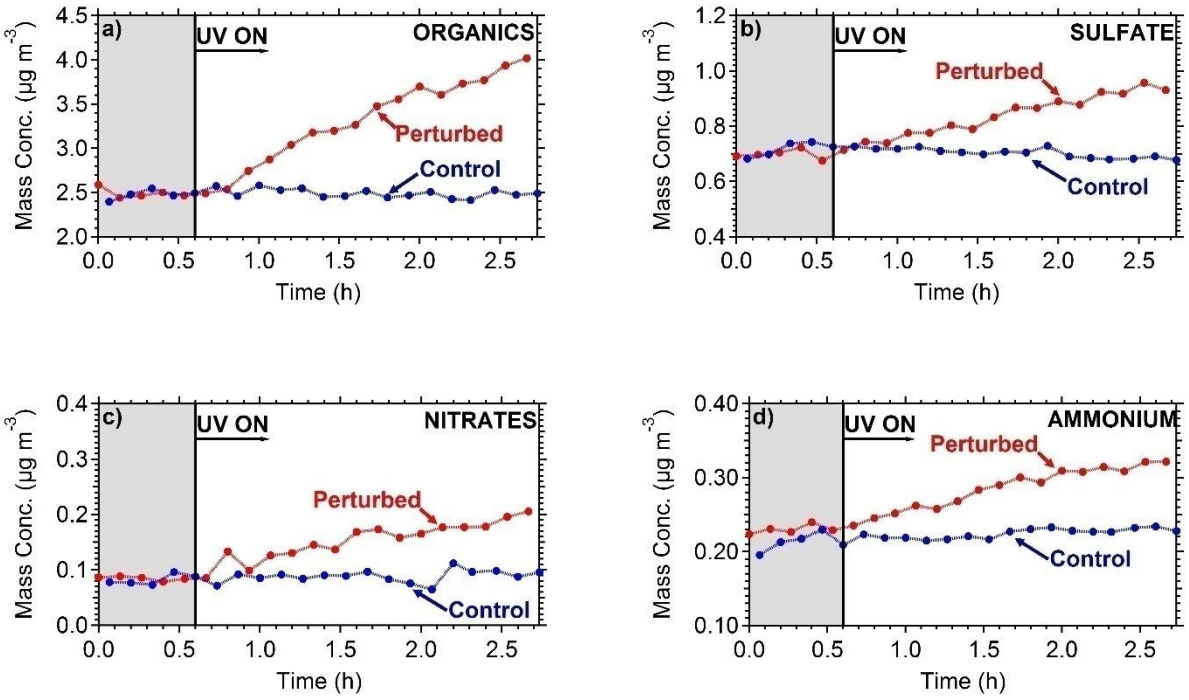

Figure 8. The particle wall-loss corrected concentrations of the major PM_1 components measured by the AMS a) organics, b) sulfate, c) nitrates and d) ammonium. The shaded area indicates that the chambers were dark. Data have been corrected for the collection efficiency (CE=0.6).

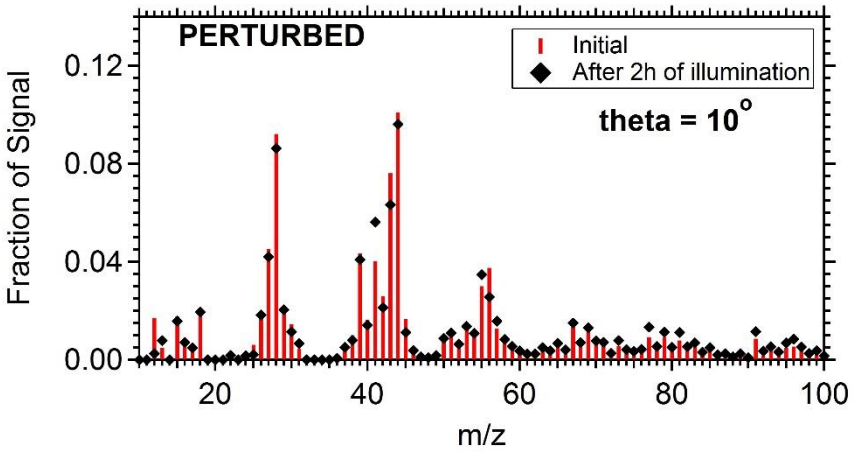

Figure 9. The organic mass spectra after filling and after two hours of UV illumination in the perturbed chamber.

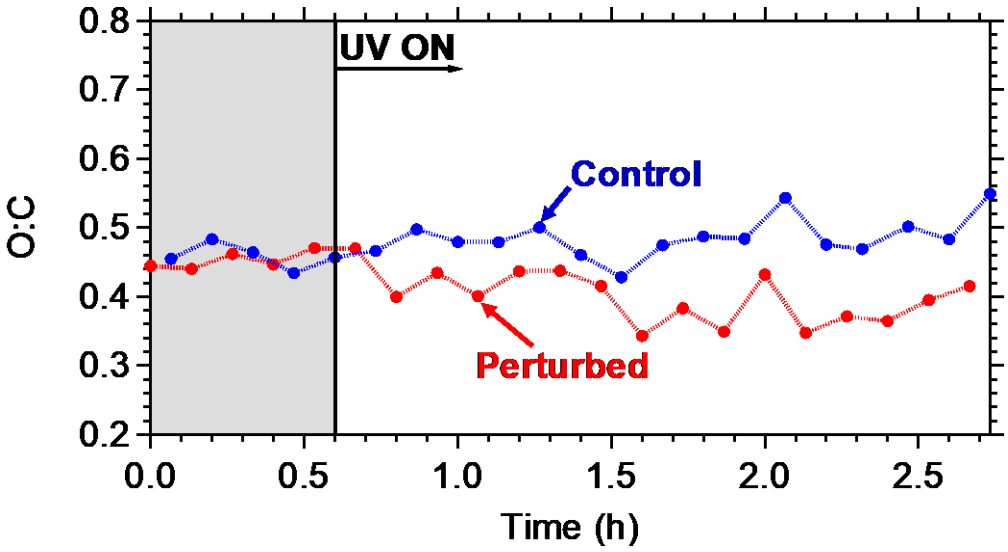

Figure 10. The O:C ratio evolution for the control and the perturbed chamber. The shaded area indicates that the chambers were in the dark.

812

813

814

815